Soft Matter

PAPER

View Article Online
View Journal | View Issue

Cite this: *Soft Matter*, 2017, **13**, 5185

Dynamical behavior of microgels of interpenetrated polymer networks

Valentina Nigro, *[ab] Roberta Angelini, [ab] Monica Bertoldo, [c] Fabio Bruni, [d] Maria Antonietta Ricci [d] and Barbara Ruzicka [ab]

Received 13th April 2017,
Accepted 13th June 2017

DOI: 10.1039/c7sm00739f

rsc.li/soft-matter-journal

Microgel suspensions of an interpenetrated Polymer Network (IPN) of PNIPAM and PAAc in D_2O have been investigated through dynamic light scattering as a function of temperature, pH and concentration across the Volume Phase Transition (VPT). The dynamics of the system is slowed down under H/D isotopic substitution due to different balance states between polymer/polymer and polymer/solvent interactions suggesting the crucial role played by H-bonding. The swelling behavior, reduced with respect to PNIPAM and water, has been described by the Flory–Rehner theory, tested for PNIPAM microgel and successfully expanded to higher order for IPN microgels. Moreover the concentration dependence of the relaxation time at neutral pH has highlighted two different routes to approach the glass transition: Arrhenius and super-Arrhenius (Vogel Fulcher Tammann) respectively below and above the VPT and a fragility plot has been derived. Fragility can be tuned by changing temperature: across the VPT particles undergo a transition from soft-strong to stiff-fragile.

1 Introduction

Research on colloidal systems has attracted great interest in the last few years, due to the variety of their technological applications and the richness of their phase behavior. Indeed they are very good model systems for understanding the general problem of dynamic arrest, since their larger tunability with respect to atomic and molecular systems[1–4] leads to complex phase diagrams, including different arrested states (such as gels[5–7] and glasses[8,9]) and unusual glass–glass transitions.[10–12]

In particular, among colloidal systems, soft colloids represent an interesting class of glass-formers, since, at variance with hardsphere-like colloids, they are characterized by an interparticle potential with a finite repulsion at or beyond contact. As a result of the particle softness a complex phase behavior has been theoretically predicted[13,14] and not yet experimentally reproduced. Moreover, it has been recently shown[15] that soft colloids exhibit the same wide variation of the structural relaxation time observed for supercooled molecular liquids approaching the glassy state. This variation is characterized by the unifying concept of fragility, which gives a "universal" description of dynamic arrest in glass-forming liquids.[16–18] The relaxation time of "fragile" liquids increases very rapidly with decreasing temperature, while "strong" liquids show a much slower temperature dependence. For colloidal suspensions fragility must be defined by replacing the inverse of temperature with concentration.[15,18,19] Hard-sphere colloidal suspensions are fragile and the absence of a wider range of fragility limits their versatility as a model system of the glass transition. Interestingly, for deformable soft colloidal particles, fragility is affected by their elastic properties, giving rise to strong behavior[16,20] and allowing obtaining the equivalent effect of molecular systems.[17] Nevertheless, many efforts have been devoted to understanding the influence of the softness of the interparticle potential on the fragility of glass formers,[18,21–23] with controversial results between computer simulations[22,23] and experimental observations.[15,24]

In this framework responsive microgels (aqueous suspensions of nanometre- or micrometre-sized hydrogel particles) allow changing their effective volume fraction and their elastic properties by tuning their response to an external stimulus. In particular, they may exhibit high sensitivity to changes of pH, temperature, electric field, ionic strength, solvent or to external stresses or light pulses. These easily accessible external parameters allow modulating the interparticle potential and their reversible Volume Phase Transition (VPT) (swelling/shrinking behavior), giving rise to novel phase-behaviors, drastically different from those of conventional hard-sphere-like colloidal systems.[25–29]

One of the most studied responsive microgels is based on a thermo-sensitive polymer, poly(*N*-isopropylacrylamide), also

[a] *Dipartimento di Fisica, Sapienza Università di Roma, P.le Aldo Moro 5, 00185 Roma, Italy. E-mail: valentina.nigro@uniroma1.it*
[b] *Istituto dei Sistemi Complessi del Consiglio Nazionale delle Ricerche (ISC-CNR), sede Sapienza, Pz.le Aldo Moro 5, I-00185 Roma, Italy*
[c] *Istituto per i Processi Chimico-Fisici del Consiglio Nazionale delle Ricerche (IPCF-CNR), Area della Ricerca, Via G.Moruzzi 1, I-56124 Pisa, Italy*
[d] *Dipartimento di Scienze, Sezione di Nanoscienze, Università degli Studi Roma Tre, Via della Vasca Navale 84, I-00146 Roma, Italy*

known as PNIPAM. Indeed PNIPAM-based microgels have been widely investigated in the last few years[30–35] and it is well known that their thermo-responsiveness is strongly related to the coil-to-globule transition with temperature of the NIPAM polymer. At room temperature indeed, the polymer is hydrophilic and strongly hydrated in solution, while it becomes hydrophobic above 305 K corresponding to its lower critical solution temperature. This gives rise to a Volume Phase Transition (VPT) from a swollen to a shrunken state of any microgel based on the NIPAM polymer.[36] Moreover, it has been shown that this typical swelling/shrinking transition is the driving mechanism of the phase behavior of aqueous suspensions of PNIPAM microgels.[15,26,28,37] This typical swelling behavior can be strongly affected by concentration,[25,38] solvents[39] and synthesis procedures (such as a growing number of cross-linking points,[40,41] different reaction pH conditions[42] or by introducing additives into the PNIPAM network[43]).

In this context PNIPAM microgels containing another species such as a co-monomer or an interpenetrated polymer are even more interesting, as a more complex scenario can show up. In particular, the addition of poly-acrilic acid (PAAc) to the PNIPAM microgel provides pH-sensitivity to the thermo-responsive microgel. The VPT of these microgels strongly depends on the effective charge density, controlled by the content of the AAc monomer,[44,45] on the pH of the suspension[46–51] and on the salt concentration.[46,52]

This means that the synthesis procedure plays a crucial role, with the response of PNIPAM/PAAc microgels being strictly related to the mutual interference between the two monomers.[52–56] While microgels made of random co-polymers (co-polymerised) have been widely investigated both experimentally and theoretically,[46,49,53,57,58] a deep investigation of Interpenetrated Polymer Network (IPN) microgels is still lacking. Interpenetration of hydrophilic PAAc into the PNIPAM microgel network (IPN PNIPAM–PAAc)[44,48,59–62] provides independent sensitivity to temperature and pH, preserving the same VPT of the pure PNIPAM microgel. Moreover the different solubilities of PAAc at acidic and neutral pH introduce an additional control parameter that allows tuning of the mutual interference between PNIPAM and PAAc networks. At acidic pH the carboxylic (COOH–) groups of PAAc chains are protonated and H-bond formation with neighbouring COOH– groups or with the amidic (CONH–) groups of PNIPAM in the same particle is favored, with respect to H-bonding with water molecules.[63] At neutral pH, the balance between PNIPAM/PAAc and water/PAAc H-bonds is reversed. Both compounds are therefore well solvated and water mediates their interaction, making the two networks completely independent from each other.

The swelling behavior of aqueous suspensions of PNIPAM–PAAc IPN microgels as a function of temperature, pH and concentration has been extensively investigated by our group and the obtained results have been published elsewhere.[50,51,64]

In order to understand the role played by hydrophobicity and hydrogen bonding in the polymer–solvent interactions and in the dynamics of the polymer solutions, investigations of the isotopic effect give relevant information. Indeed it has been recently shown that slowing down of the swelling kinetics and a shift forward of the Volume Phase Transition Temperature (VPTT) of PNIPAM microgels occur in D_2O suspensions with respect to H_2O ones,[65] mainly due to the higher viscosity of the deuterated solvent. Similar results have been found also in other colloidal suspensions.[66–68]

In this work we present a DLS systematic investigation of the dynamics across the VPT of IPN microgel suspensions in D_2O compared to H_2O as a function of temperature, pH and concentration. Experimental data have been described through theoretical models from the Flory–Rehner theory and discussed within the universal framework of fragility.

2 Experimental methods

2.1 Sample preparation

Once synthesized by a sequential free radical polymerization method, lyophilized IPN microgels were dispersed in H_2O or D_2O under magnetic stirring for 1 day. The samples were then lyophilized and redispersed in H_2O or D_2O using the same molar ratio; the weight concentration, C_w, reported in the text always refers to the case of H_2O. Samples at different concentrations were obtained by dilution at two pH values: pH 5, where H-bondings between PNIPAM and PAAc are favored, and pH 7, corresponding to the dissociation of the ionic groups and the reduction of the PNIPAM–PAAc H-bond interactions. Samples at pH 7 were obtained by the addition of NaOH or NaOD to the samples at pH 5. A detailed description of IPN microgel particle synthesis is reported in ref. 50 and 51.

2.2 DLS set-up and data analysis

Fig. 1 shows the typical behavior of the normalized intensity autocorrelation functions for an IPN sample at weight concentrations

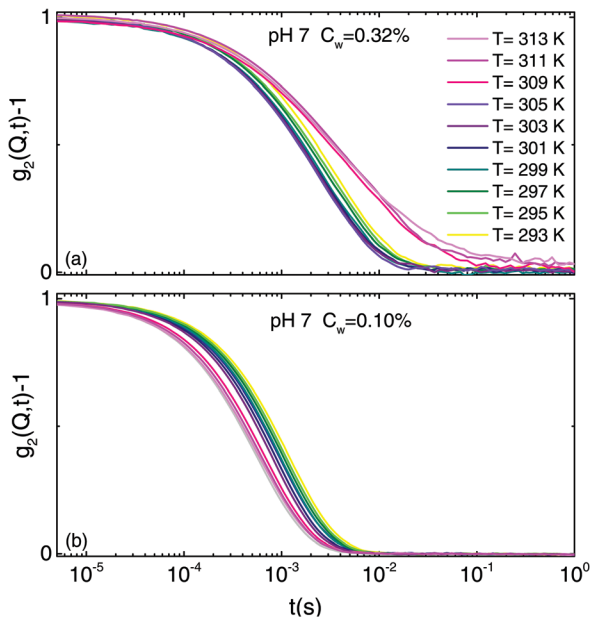

Fig. 1 Normalized intensity autocorrelation function of a D_2O suspension of IPN microgels at (a) C_w = 0.32% and (b) C_w = 0.10%, at pH 7 and Q = 1.8×10^{-2} nm^{-1} for the indicated temperatures.

C_w = 0.32% (Fig. 1(a)) and C_w = 0.10% (Fig. 1(b)) and pH 7, collected at $Q = 1.8 \times 10^{-2}$ nm^{-1}.

DLS measurements have been performed with a multiangle light scattering setup. The monochromatic and polarized beam emitted from a solid state laser (100 mW at λ = 642 nm) is focused on the sample placed in a cylindrical VAT for index matching and temperature control. The scattered intensity is simultaneously collected at five different scattering angles, namely θ = 30°, 50°, 70°, 90°, 110°, corresponding to the five scattering vectors Q ($Q = 0.67 \times 10^{-2}$ nm^{-1}, 1.1×10^{-2} nm^{-1}, 1.5×10^{-2} nm^{-1}, 1.8×10^{-2} nm^{-1}, 2.1×10^{-2} nm^{-1}), according to the relation $Q = (4\pi n/\lambda)\sin(\theta/2)$. Single mode optical fibers coupled to collimators collect the scattered light as a function of time and scattering vector. In this way one can simultaneously measure the normalized intensity autocorrelation function $g_2(Q,t) = \langle I(Q,t)I(Q,0)\rangle/\langle I(Q,0)\rangle^2$ at five different Q values with a high coherence factor close to the ideal unit value. Measurements have been performed as a function of temperature in the range T = (293–313) K across the VPT at four different weight concentrations (C_w = 0.10%, C_w = 0.15%, C_w = 0.20%, and C_w = 0.32%), at both acidic and neutral pH. Reproducibility has been tested by repeating measurements several times.

As commonly known, the intensity correlation function of most colloidal systems is well described by the Kohlrausch–Williams–Watts expression:[69,70]

$$g_2(Q,t) = 1 + b[(e^{-t/\tau})^{\beta}]^2 \quad (1)$$

where b is the coherence factor, τ is an "effective" relaxation time and β describes the deviation from the simple exponential decay (β = 1) usually found in monodisperse systems and gives a measure of the distribution of relaxation times. Many glassy materials show a stretching of the correlation functions (here referred to as "stretched behavior") characterized by an exponent $\beta < 1$.

3 Results

3.1 Isotopic effect on the dynamics

In Fig. 2 the comparison between the temperature dependence of the relaxation time and the β parameter, as obtained through a fit with eqn (1), for D_2O and H_2O suspensions, at (a) pH 5 and (b) pH 7, is reported at two fixed concentrations as an example. In D_2O a dynamical transition associated with the VPT, from a swollen to a shrunken state, is evidenced as for H_2O suspensions.[50] At acidic pH (Fig. 2(a)) the relaxation time slightly decreases as the temperature increases, until the transition, evidenced by a change in the slope, is approached around T = 305 K for H_2O and T = 307 K for D_2O. Above this temperature the relaxation time decreases to its lowest value, corresponding to the shrunken state. Moreover the stretching parameter β (inset of Fig. 2(a)) is almost constant with temperature and concentration and indicates slightly stretched correlation functions ($\beta \approx 0.9$).

This behavior is strongly affected by the pH of the solution, as shown in Fig. 2(b): at pH 7 the relaxation time slowly decreases as the temperature increases up to the VPTT as for pH 5; above this temperature the relaxation time of low concentrated samples (C_w = 0.15%) decreases, whilst that of the samples at high concentration (C_w = 0.32%) increases. This effect is well enhanced in D_2O. At the same time the stretching parameter β, at variance with the case of pH 5, decreases with concentrations showing a step across the VPTT. As for the relaxation time at the highest concentration in D_2O β shows a significant jump to lower values (inset of Fig. 2(b)), corresponding to a clear change of the shape of the intensity autocorrelation functions, well evidenced in Fig. 1(a). Interestingly this peculiar behavior both for τ and β can be interpreted as the first evidence of an aggregation phenomenon and as a precursor of the transition from an ergodic to a non-ergodic state expected at even higher concentrations.

Although the main features of the typical swelling behavior in H_2O suspensions[50] are preserved under isotopic substitution, interesting differences between D_2O and H_2O samples are observed. As evidenced in Fig. 2, the relaxation times are always higher in D_2O than in H_2O, at all pH values and concentrations, suggesting a slowing down of the dynamics under isotopic substitution, probably due to the higher viscosity of D_2O than H_2O. Moreover, at pH 5 a shift of the VPTT to higher temperature with respect to H_2O is observed, in agreement with that found for PNIPAM microgel suspensions.[65] On the contrary, at pH 7 the VPT occurs at the same temperature in both solvents, confirming that pH affects the role played by H-bonding. Finally, at neutral pH and at the highest concentration the jump of the relaxation time to higher values above the VPTT is greatly amplified under H/D isotopic substitution on the solvent, as evidenced in Fig. 2(b). The β parameter is significantly affected by isotopic substitution only for the highest concentration at pH 7, as evident from its lower values and the jump across the VPTT. This may suggest that aggregation is promoted in the D_2O solvent at neutral pH, since the slowing down of the dynamics and the reduction of the mutual interference between PNIPAM and PAAc networks drive the system to arrest.

In order to obtain additional information on the dynamical behavior of D_2O IPN microgel suspensions, the relaxation time and the stretching parameter have been investigated at different length scales, as a function of the scattering vector Q well below the peak position of the static structure factor at $Q \sim 0.08$ nm^{-1}, as obtained from SAXS measurements in the Q-range 0.015–0.5 nm^{-1} at T = (293–313) K and with an incident X-ray energy fixed at 12.4 keV. In Fig. 3, the Q-dependence of the relaxation time at C_w = 0.20% at pH 5 and pH 7, is reported as an example. It can be described by a typical power law decay:

$$\tau = AQ^{-n} \quad (2)$$

where A is a constant and the exponent n defines the nature of the motion. The fits according to eqn (2) are superimposed to the data as full or dashed lines in Fig. 3. The mean exponents $\bar{n}$ are $\bar{n}_{pH5} = 2.3 \pm 0.1$ and $\bar{n}_{pH7} = 2.9 \pm 0.1$ in agreement with measurements on IPN microgel suspensions in H_2O.[50] This peculiar behavior may be due to the complex morphology of IPN microgel particles, with a highly cross-linked core and a less crosslinked corona, which may affect the dynamics. Moreover concentration and temperature

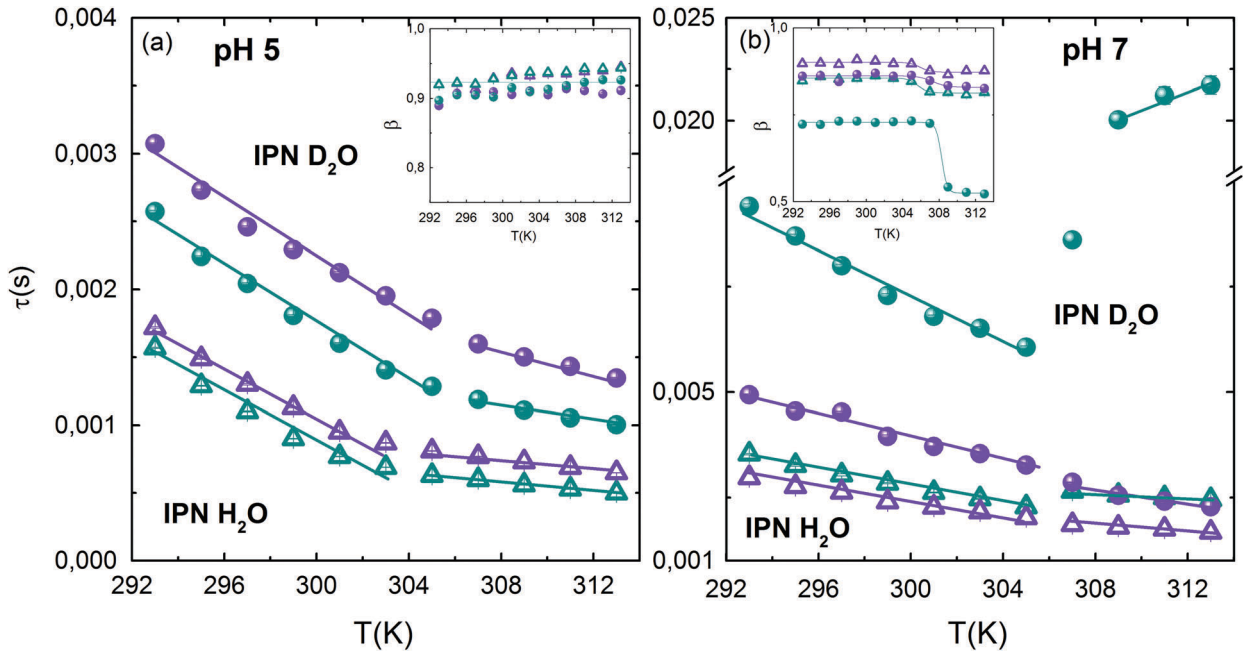

Fig. 2 Relaxation time and stretching parameter (inset) as a function of temperature for D_2O (circles) and H_2O (triangles) suspensions of IPN microgels at C_w = 0.15% (violet) and C_w = 0.32% (cyan) at (a) pH 5 and (b) pH 7 for $Q = 1.8 \times 10^{-2}$ nm^{-1}. Full lines are guides to the eyes.

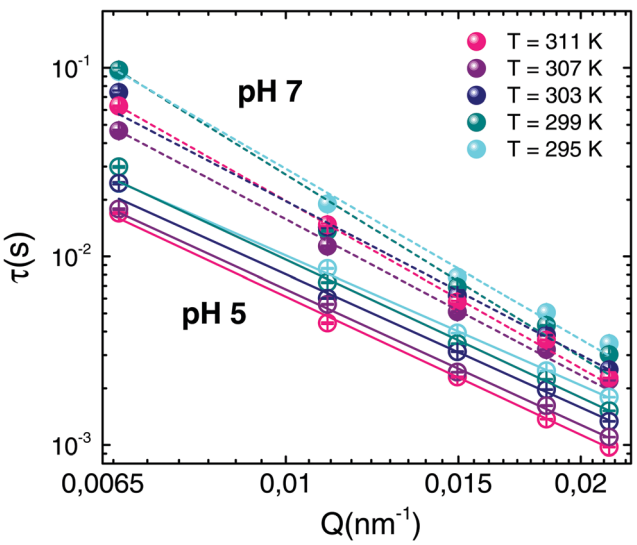

Fig. 3 Relaxation time as a function of scattering vector Q at C_w = 0.20% in D_2O at pH 5 and pH 7 for the indicated temperatures. Full (pH 5) and dashed (pH 7) lines are fits through eqn (2) with $\bar{n}_{pH5} = 2.3 \pm 0.1$ and $\bar{n}_{pH7} = 2.9 \pm 0.1$.

do not significantly affect the Q dependence of the relaxation time. Similar results have already been published for different polymers[71,72] and responsive microgels,[73] although a theoretical explanation is not yet available. Meanwhile the stretching parameter β does not show any dependence on the scattering vector Q as observed in H_2O suspensions.[50]

3.2 Swelling behavior and a theoretical model

The temperature dependence of the normalized hydrodynamic radii of IPN microgels in both H_2O and D_2O suspensions is shown in Fig. 4(a) at acidic pH and in Fig. 4(b) at neutral pH and compared with PNIPAM microgels at the same weight concentration (C_w = 0.10%). The radii have been calculated, according to the Stokes–Einsteins relation for Brownian particles in the high dilution limit, as $R = k_BT/6\pi\eta D$, where D is the translational diffusion coefficient calculated from τ through the relation $\tau = 1/Q^2D$. The sample viscosity η has been approximated with the solvent one and the radii have been normalized with respect to their values at T = 297 K reported in the caption of Fig. 4. Fig. 4 evidences a clear reduction of the normalized radii of IPN microgels in both solvents compared to the PNIPAM microgel, thus confirming that the presence of poly(acrylic acid) reduces the swelling capability of the microgel particles also in deuterated suspensions.[44,48,49] Nevertheless different behaviors depending on solvent and pH are observed. For D_2O suspensions at acidic pH the range of variability of R is reduced with respect to H_2O, while at neutral pH the transition is smoother than in H_2O. Moreover, while in H_2O a clear difference is observed between the temperature behavior of the normalized radii at acidic and neutral pH, no significant changes are evident in D_2O. This suggests that the balance between polymer/polymer and polymer/solvent interactions strictly depends on the solvent and therefore on the H-bonds.

The swelling behavior of microgels has been widely described *via* the Flory–Rehner theory[74] which gives the equation of state under the equilibrium conditions:

$$\ln(1-\phi) + \phi + \chi\phi^2 + \frac{\phi_0}{N}\left[\left(\frac{\phi}{\phi_0}\right)^{1/3} - \frac{1}{2}\frac{\phi}{\phi_0}\right] = 0 \qquad (3)$$

ϕ is the polymer volume fraction within the particle and ϕ_0 is the polymer volume fraction in the reference state, typically

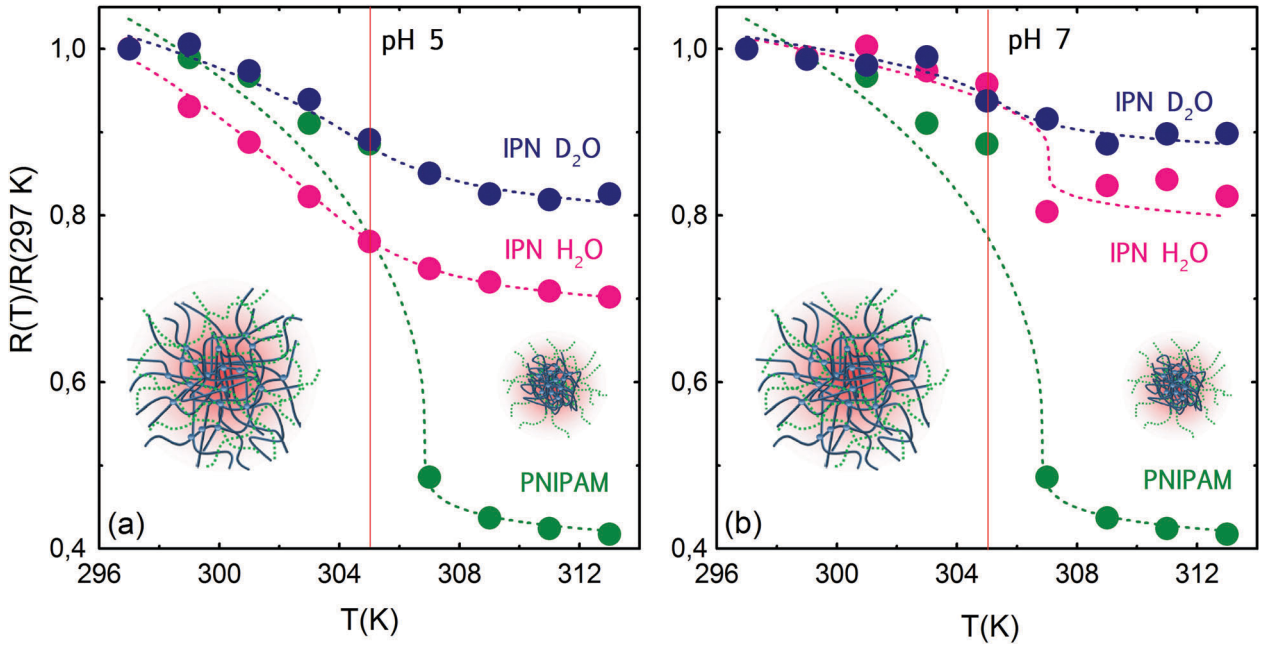

Fig. 4 Normalized radius as obtained from DLS measurements for an IPN microgel in both H_2O and D_2O suspensions at C_w = 0.10%, $Q = 1.8 \times 10^{-2}$ nm^{-1} and (a) pH 5 and (b) pH 7, compared with the normalized radius obtained for PNIPAM microgels. The hydrodynamic radii have been normalized at the corresponding values at T = 297 K: R_{PNIPAM} = (55.1 ± 0.2) nm; $R_{IPN\,H_2O\,pH5}$ = (97.7 ± 0.3) nm; $R_{IPN\,D_2O\,pH5}$ = (95.7 ± 0.4) nm; $R_{IPN\,H_2O\,pH7}$ = (135.7 ± 0.5) nm and $R_{IPN\,D_2O\,pH7}$ = (119.1 ± 0.3) nm. Dashed lines are the best fits through the modified Flory–Rehner theory as explained in the text.

taken as the shrunken one. For isotropic swelling, ϕ can be related to the particle size R as

$$\frac{\phi}{\phi_0} = \left(\frac{R_0}{R}\right)^3 \tag{4}$$

where R_0 is the particle diameter in the reference state and R is the particle diameter in a given state. N is the average number of segments between two neighboring cross-linking points in the gel network and χ is the Flory polymer–solvent energy parameter that can be written as a power series expansion:

$$\chi = \chi_1(T) + \chi_2\phi + \chi_3\phi^2 + \chi_4\phi^3 + \cdots \tag{5}$$

where χ_1 is the Flory parameter and χ_2, χ_3, χ_4,... are temperature independent coefficients that introduce additional terms in the equation of state (eqn (3)). This model well describes the VPT in the case of pure PNIPAM microgels as shown in Fig. 4(a) where a second-order approximation of eqn (5) is considered. However, it does not reproduce the discontinuous transition observed in other soft colloidal microgels where exchange interactions must be taken into account considering higher order interactions than contacts between molecules.[64,75,76] Therefore for IPN microgels a careful choice of the order approximation of $\chi(\phi)$ is required. Indeed for IPN in H_2O at acidic pH the best fit of our experimental data is obtained *via* a second-order approximation of eqn (5), such as for PNIPAM microgels. On the contrary, for H_2O samples at neutral pH and for D_2O samples at both acidic and neutral pH, a third-order approximation is needed for good agreement between theory and experiments. This comparison has recently provided details about the delicate balance between energetic and entropic contribution assuming that χ is an effective mean parameter accounting for polymer/polymer interactions within each network, polymer/polymer interactions between different networks and polymer/solvent interactions. We have indeed observed that the swelling process in H_2O is more favored at acidic than neutral pH, with the system being more hydrophobic. Moreover it hugely depends on solvent: in D_2O the pH influence is less significant than in H_2O, confirming that the balance between polymer/polymer and polymer/solvent interactions strictly depends on the solvent and therefore on H-bonding.[64]

3.3 Fragility in H_2O and D_2O suspensions of IPN microgels

It is well known that in supercooled molecular liquids the structural relaxation time and the viscosity grow many orders of magnitude with decreasing temperature when the glassy state is approached.[16] The rapidity with which these quantities increase can be quantified by the fragility index m defined as

$$m = \left[\frac{\partial \log \tau}{\partial (T_g/T)}\right]_{T=T_g} \tag{6}$$

where τ is the relaxation time and T_g is the glass transition temperature. In "fragile" liquids the relaxation time and viscosity are highly sensitive to changes in T with a super-Arrhenius (Vogel Fulcher Tammann) behavior, while in "strong" liquids they have a much lower T sensitivity with an Arrhenius dependence. This unifying concept describes and classifies the behavior of glass forming systems.[16,17,77] The same concept has been extended to colloids where the glass transition occurs by

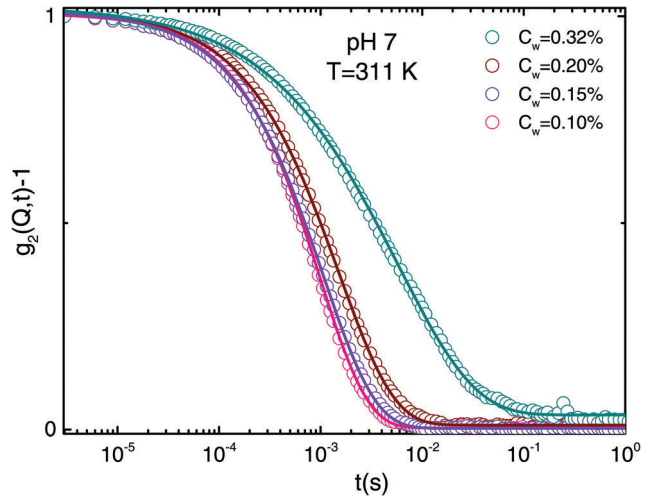

Fig. 5 Normalized intensity autocorrelation functions of a D_2O suspension of IPN microgels at fixed temperature (T = 311 K), pH 7 and Q = 1.8 × 10^{-2} nm^{-1} for the indicated concentrations. Lines superimposed to data are fits according to eqn (1).

increasing the volume fraction.[15,18] A recent work on IPN microgel suspensions in water at different concentrations and fixed temperature has related the fragility of soft colloidal particles to their elastic properties.[15]

In this work we perform an extensive investigation at different concentrations, temperatures and solvents. The concentration dependence of the dynamics of IPN microgel suspensions is highlighted in Fig. 5, where the normalized intensity autocorrelation functions at fixed temperature (T = 311 K) and pH 7 are reported. The observed behavior indicates that as the concentration increases, the decay becomes more and more stretched, as well evidenced in Fig. 6, where the concentration behavior of the stretching parameter β at fixed temperatures (T = 295 K and T = 311 K) and pH 7, is

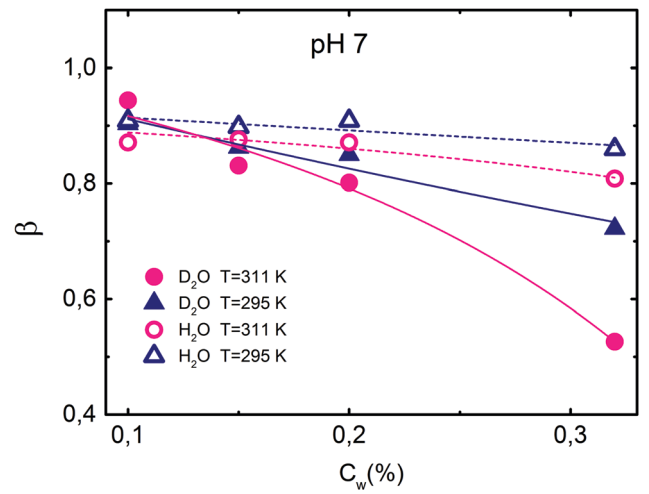

Fig. 6 Stretching coefficient as obtained from normalized intensity autocorrelation functions for D_2O and H_2O suspensions of IPN microgels at fixed temperature (T = 311 K), pH 7 and Q = 1.8 × 10^{-2} nm^{-1} for the indicated concentrations. Full (D_2O) and dashed (H_2O) lines are Arrhenius fits for T < VPTT and Vogel–Fulcher–Tamman fits for T > VPTT.

reported for both D_2O and H_2O suspensions. We find that β decreases with concentration showing an enhancement in the case of D_2O above the VPTT (T = 311 K).

The comparison between the concentration dependence of the relaxation time at acidic and neutral pH is reported in Fig. 7(a) and (b). At pH 5 τ linearly decreases as the concentration increases indicating a slight fastening of the dynamics while at pH 7 it exhibits an inverted trend with an exponential growth with different sensitivities to concentration below and above the VPT, suggesting the existence of two different routes to approach the glass transition. Moreover a faster rise at the highest temperature (T = 311 K) indicates the appearance of an aggregation phenomenon. The different behaviors observed in the investigated concentration range at pH 5 and pH 7 implies that the presence of PAAc, with respect to pure PNIPAM, hugely affects the dynamics of the system. The concentration decrease of the relaxation time at acidic pH is consistent with theoretical studies that predict an increase with concentrations of the diffusion coefficient[78–80] on charged colloidal particles. This indicates that the electrostatic effect plays an important role in the dynamics of the studied IPN microgels. New scenarios could appear at higher concentrations. The reversed behavior observed at neutral pH can be related to intervening short-range attractive interactions due to hydrogen bonding between deprotonated carboxylic groups of PAAc chains belonging to distinct particles. Indeed, the ionization of PAAc at increasing pH corresponds to a transition from an insoluble to a soluble state of the polymeric chains and even if the interconnection of PAAc in the PNIPAM network avoids its diffusion out of particles, it cannot avoid the interaction between the freely moving chain-end segments at the particle surface. A deeper investigation on the charge of the system is in progress, to shed light on the relevance of the electrostatic effect on the dynamics.

Indeed we found that below the VPT the data are well fitted with an Arrhenius behavior, typically observed in strong molecular glass-formers, where C_w plays the role of $1/T$. Therefore at these temperatures data are well described by the relation

$$\tau = \tau_0 e^{AC_w} \quad (7)$$

where A is a constant and τ_0 is the characteristic relaxation time for low values of C_w. On the other hand above the VPT, data are strongly dependent on the concentration, cannot be described through a simple Arrhenius model and a super-Arrhenius behavior as the Vogel–Fulcher–Tammann (VFT) has to be considered:

$$\tau = \tau_0 e^{\frac{\bar{A}C_w}{C_0 - C_w}} \quad (8)$$

where C_0 sets the apparent divergence, $\bar{A}$ controls the growth of the relaxation time on approaching C_0 and τ_0 is the characteristic relaxation time at low concentrations. These functions provide a good description of the concentration dependence of τ and β as shown in Fig. 6 and 7, thus confirming that the paradigm for supercooled molecular liquids near their glass transition can be extended to suspensions of soft particles, where the concentration C_w plays a role analogous to the inverse of temperature $1/T$ in molecular systems.

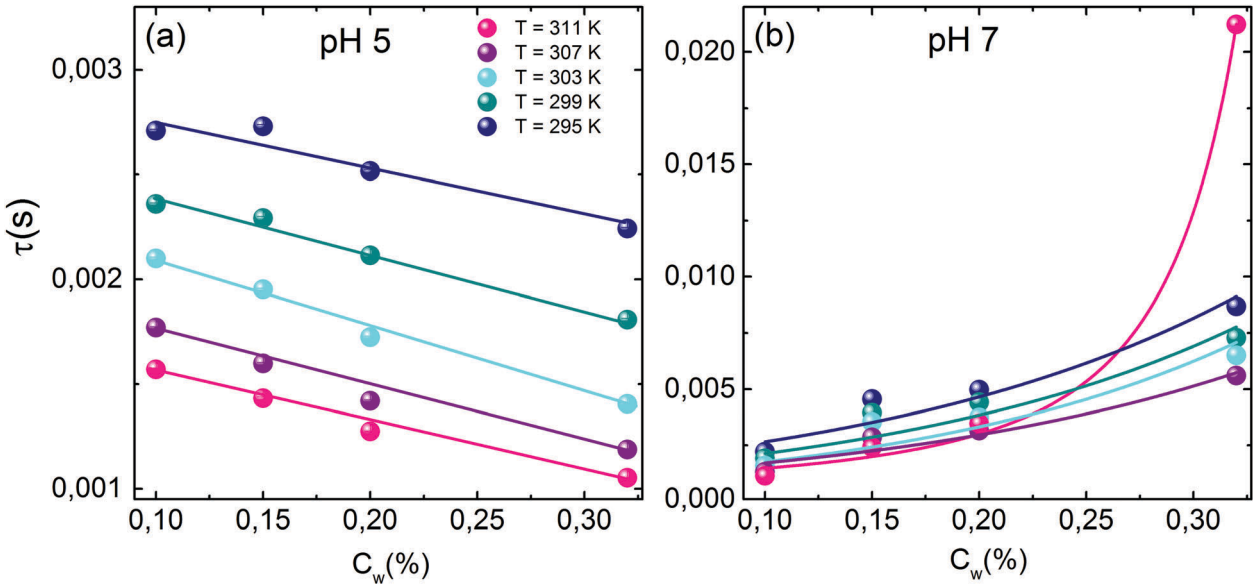

Fig. 7 Relaxation times as a function of weight concentration at fixed temperatures at (a) pH 5 and (b) pH 7 for D_2O suspensions at $Q = 1.8 \times 10^{-2}$ nm^{-1}. Full lines in (a) are linear fits and full lines in (b) are fits according to eqn (7) below the VPTT and eqn (8) above the VPTT.

Generally the concept of fragility is summarized in a renormalized Arrhenius plot, where the temperature is rescaled by the glass transition temperature, T_g, and fragility is defined by the logarithmic slope at T_g.[16] This representation provides a unifying framework to describe the variation from strong to fragile behavior of molecular liquids. According to Mattsson *et al.*,[15] we explore the analogy between soft colloidal suspensions and molecular glass-formers by rescaling the Arrhenius plot in a fashion similar to that used for molecular glasses. Indeed the corresponding plot for colloids can be obtained by scaling C_w by the "glass concentration" C_g, defined as the concentration $C_w(\tau = 100\ \text{s})$, where the structural relaxation time is no longer experimentally accessible.[17] In this way we obtain a renormalized Arrhenius plot for D_2O and H_2O suspensions, as shown in Fig. 8 at pH 7, where only two temperatures are reported since all data below the VPTT collapse at $T = 295$ K and all data above collapse at $T = 311$ K. The slope of the data at $C_w = C_g$ defines the fragility:

$$m = \left[\frac{\partial \log \tau}{\partial (C_w/C_g)}\right]_{C_w = C_g} \quad (9)$$

As discussed before the most fragile materials are those that show the largest deviations from the Arrhenius law. In our case we observe that both in D_2O and H_2O for all temperatures below the VPT, in the swollen state, soft IPN microgels behave as strong materials. On the contrary, at temperatures above the VPT, in the shrunken state, they become stiff and behave as fragile systems. Moreover in this case the fragility of the system can be tuned by changing the solvent. In particular for all $T <$ VPTT we find $m \approx 5$ in both H_2O and D_2O suspensions and for all $T >$ VPTT, we find $m \approx 30$ in H_2O and $m \approx 40$ in D_2O, where higher values of m correspond to stiffer particles. This means that across the VPT the system encompasses a transition

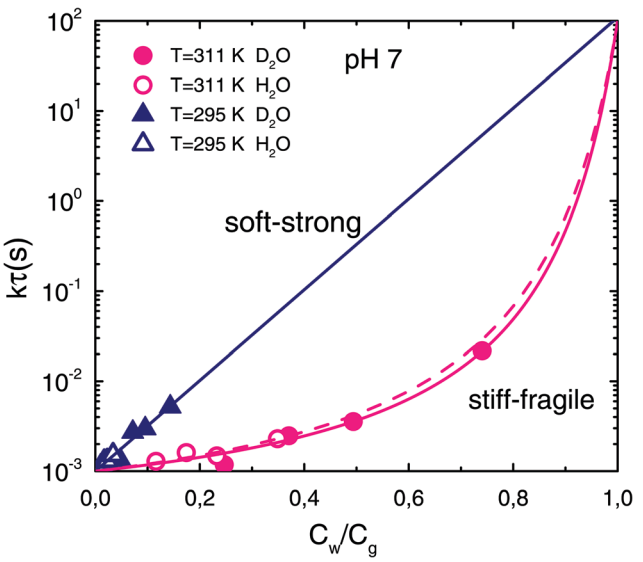

Fig. 8 Arrhenius plot for the scaled relaxation time $k\tau$ with $k = 10^{-3}/\tau_0$ *versus* concentration C_w normalized by $C_g = C_w(\tau(100\ \text{s}))$ at $T = 295$ K (triangles) and $T = 311$ K (circles) for D_2O (solid symbols) and H_2O (open symbols). Lines superimposed to data are fits according to the Arrhenius (black line) and the VFT (magenta line) equations, for soft and stiff particles, respectively.

from a strong to a fragile behavior in both solvents. Nevertheless we find that above the VPT, microgel particles in D_2O suspensions are stiffer than in H_2O, thus leading to a more fragile behavior. Interestingly, this observation is reminiscent of what is seen for the concentration dependence of β, where lower values correspond to stiffer particles and therefore to more fragile behaviors. At variance with previous studies, where the fragility of the particles was varied by changing the polymeric networks, here we are able to pass from a strong (soft) to

fragile (stiff) behavior on a single system by changing temperature below and above the VPT.

These findings confirm that the fragility of colloidal particles increases as softness decreases, according to the experimental results by Mattsson *et al.*[15] Moreover our study is extended to different temperatures and solvents providing the possibility of modulating the inherent softness of microgel particles and therefore their fragility. This point, still controversial, calls for further experimental, numerical and theoretical investigations.

4 Conclusions

The swelling behavior of PNIPAM–PAAc IPN microgels has been investigated as a function of temperature, solvent, pH, concentration and scattering vector by comparing new experiments on deuterated suspensions with previous findings on IPN microgels in H_2O.[50]

It has been shown that H/D isotopic substitution in the solvent plays an important role in the kinetics of the swelling although preserving the same physical properties observed in H_2O. This suggests that hydrogen-bonds play a crucial role in the polymer–solvent interactions and that the swelling kinetics can be slightly affected by isotopic substitution. In this case, indeed, stronger H-bonding occurs between the polymer and the solvent with respect to the case of H_2O with consequent changes in the rate of the swelling/shrinking transition.[65]

Moreover the dynamics of IPN microgels is slowed down in the D_2O solvent. Importantly for the highest concentration at pH 7 a clear enhanced transition of the relaxation time above the VPTT compared to H_2O is found. This behavior can be interpreted as a precursor of a non-ergodic transition expected at even higher concentrations.

Experimental data have been compared with theoretical models from the Flory–Rehner theory: while PNIPAM microgel data are well described through the second order approximation of the Flory parameter $\chi(\phi)$, for IPN microgels under neutral conditions and in D_2O solvents we extended the model by considering a third-order contribution.

Finally, applying to colloidal systems the universal framework of fragility,[15] we find that the elastic response of IPN microgel suspensions can be modulated by changing temperature: below the VPT particles are soft and deformable, whilst above the VPT they become stiff and undeformable. This is associated with increasing values of fragility, which suggests that the swelling/shriking behavior drives the system through a transition from strong to fragile. Therefore fragility has to be strictly related to the VPT: soft particles will lead to strong behavior and stiff particles to fragile behavior.

Acknowledgements

The authors acknowledge support from the European Research Council (ERC Consolidator Grant 681597, MIMIC) and from MIUR-PRIN (2012J8X57P).

References

1 F. Sciortino and P. Tartaglia, *Adv. Phys.*, 2005, **54**, 471–524.
2 V. Trappe and P. Sandkühler, *Curr. Opin. Colloid Interface Sci.*, 2004, **8**, 494–500.
3 W. C. K. Poon, *Curr. Opin. Colloid Interface Sci.*, 1998, **3**, 593–599.
4 E. Zaccarelli, *J. Phys.: Condens. Matter*, 2008, **20**, 494242.
5 P. J. Lu, E. Zaccarelli, F. Ciulla, A. B. Schofield, F. Sciortino and D. A. Weitz, *Nature*, 2008, **453**, 499–503.
6 C. P. Royall, S. R. Williams, T. Ohtsuka and H. Tanaka, *Nat. Mater.*, 2008, **7**, 556–561.
7 B. Ruzicka, E. Zaccarelli, L. Zulian, R. Angelini, M. Sztucki, A. Moussaïd, T. Narayanan and F. Sciortino, *Nat. Mater.*, 2011, **10**, 56–60.
8 P. N. Pusey and W. van Megen, *Nature*, 1986, **320**, 340–342.
9 A. Imhof and J. K. G. Dhont, *Phys. Rev. Lett.*, 1995, **75**, 1662–1665.
10 K. N. Pham, A. M. Puertas, J. Bergenholtz, S. U. Egelhaaf, A. Moussaïd, P. N. Pusey, A. B. Schofield, M. E. Cates, M. Fuchs and W. C. K. Poon, *Science*, 2002, **296**, 104–106.
11 T. Eckert and E. Bartsch, *Phys. Rev. Lett.*, 2002, **89**, 125701.
12 R. Angelini, E. Zaccarelli, F. A. de Melo Marques, M. Sztucki, A. Fluerasu, G. Ruocco and B. Ruzicka, *Nat. Commun.*, 2014, **5**, 4049.
13 C. N. Likos, N. Hoffmann, H. Löwen and A. A. Louis, *J. Phys.: Condens. Matter*, 2002, **14**, 7681–7698.
14 P. E. Ramírez-González and M. Medina-Noyola, *J. Phys.: Condens. Matter*, 2009, **21**, 075101.
15 J. Mattsson, H. M. Wyss, A. Fernandez-Nieves, K. Miyazaki, Z. Hu, D. Reichman and D. A. Weitz, *Nature*, 2009, **462**, 83–86.
16 C. Angell, *Proc. Natl. Acad. Sci. U. S. A.*, 1995, **92**, 6675–6682.
17 C. Angell, K. L. Ngai, G. B. McKenna, P. F. McMillan and S. W. Martin, *J. Appl. Phys.*, 2000, **88**, 3113–3157.
18 R. Casalini, *J. Chem. Phys.*, 2012, **137**, 204904.
19 X. Peng and G. B. McKenna, *Phys. Rev. E*, 2016, **93**, 042603.
20 R. P. Seekell, P. S. Sarangapani, Z. Zhangb and Y. Zhu, *Soft Matter*, 2015, **11**, 5485–5491.
21 P. Bordat, F. Affouard and M. Descamps, *Phys. Rev. Lett.*, 2004, **93**, 105502.
22 S. Sengupta, F. Vasconcelos, F. Affouard and S. Sastry, *J. Chem. Phys.*, 2011, **135**, 194503.
23 Z. Shi, P. G. Debenedetti, F. H. Stillinger and P. Ginart, *J. Chem. Phys.*, 2011, **135**, 084153.
24 X. Di, X. Peng and G. B. McKenna, *J. Chem. Phys.*, 2014, **140**, 054903.
25 H. Wang, X. Wu, Z. Zhu, C. S. Liu and Z. Zhang, *J. Chem. Phys.*, 2014, **140**, 024908.
26 P. S. Mohanty, D. Paloli, J. J. Crassous, E. Zaccarelli and P. Schurtenberger, *J. Chem. Phys.*, 2014, **140**, 094901.
27 T. Hellweg, C. Dewhurst, E. Brückner, K. Kratz and W. Eimer, *Colloid Polym. Sci.*, 2000, **278**, 972–978.
28 D. Paloli, P. S. Mohanty, J. J. Crassous, E. Zaccarelli and P. Schurtenberger, *Soft Matter*, 2013, **9**, 3000–3004.
29 J. Wu, B. Zhou and Z. Hu, *Phys. Rev. Lett.*, 2003, **90**, 048304.

30 R. H. Pelton and P. Chibante, *Colloids Surf.*, 1986, **20**, 247–256.
31 B. R. Saunders and B. Vincent, *Adv. Colloid Interface Sci.*, 1999, **80**, 1–25.
32 R. H. Pelton, *Adv. Colloid Interface Sci.*, 2000, **85**, 1–33.
33 M. Das, H. Zhang and E. Kumacheva, *Annu. Rev. Mater. Res.*, 2006, **36**, 117–142.
34 M. Karg and T. Hellweg, *Curr. Opin. Colloid Interface Sci.*, 2009, **14**, 438–450.
35 Y. Lu and M. Ballauff, *Prog. Polym. Sci.*, 2011, **36**, 767–792.
36 J. Wu, G. Huang and Z. Hu, *Macromolecules*, 2003, **36**, 440–448.
37 L. A. Lyon and A. Fernandez-Nieves, *Annu. Rev. Phys. Chem.*, 2012, **63**, 25–43.
38 B. H. Tan, R. H. Pelton and K. C. Tam, *Polymers*, 2010, **51**, 3238–3243.
39 P. W. Zhu and D. H. Napper, *Macromol. Chem. Phys.*, 1999, **200**, 1950–1955.
40 K. Kratz and W. Eimer, *Ber. Bunsenges. Phys. Chem.*, 1998, **102**, 848–854.
41 K. Kratz, T. Hellweg and W. Eimer, *Polymer*, 2001, **42**, 6631–6639.
42 L. Bao and L. Zhaj, *J. Macromol. Sci., Part A: Pure Appl. Chem.*, 2006, **43**, 1765–1771.
43 T. Hellweg, C. D. Dewhurst, W. Eimer and K. Kratz, *Langmuir*, 2004, **20**, 4333–4335.
44 Z. Hu and X. Xia, *Adv. Mater.*, 2004, **16**, 305–309.
45 J. Ma, B. Fan, B. Liang and J. Xu, *J. Colloid Interface Sci.*, 2010, **341**, 88–93.
46 K. Kratz, T. Hellweg and W. Eimer, *Colloids Surf., A*, 2000, **170**, 137–149.
47 K. Kratz, T. Hellweg and W. Eimer, *Ber. Bunsenges. Phys. Chem.*, 1998, **102**, 1603–1608.
48 X. Xia and Z. Hu, *Langmuir*, 2004, **20**, 2094–2098.
49 C. D. Jones and L. A. Lyon, *Macromolecules*, 2000, **33**, 8301–8303.
50 V. Nigro, R. Angelini, M. Bertoldo, V. Castelvetro, G. Ruocco and B. Ruzicka, *J. Non-Cryst. Solids*, 2015, **407**, 361–366.
51 V. Nigro, R. Angelini, M. Bertoldo, F. Bruni, M. Ricci and B. Ruzicka, *J. Chem. Phys.*, 2015, **143**, 114904.
52 W. Xiong, X. Gao, Y. Zao, H. Xu and X. Yang, *Colloids Surf. B: Biointerfaces*, 2011, **84**, 103–110.
53 Z. Meng, J. K. Cho, S. Debord, V. Breedveld and L. A. Lyon, *J. Phys. Chem. B*, 2007, **111**, 6992–6997.
54 L. A. Lyon, J. D. Debord, S. B. Debord, C. D. Jones, J. G. McGrath and M. J. Serpe, *J. Phys. Chem. B*, 2004, **108**, 19099–19108.
55 P. Holmqvist, P. S. Mohanty, G. Nägele, P. Schurtenberger and M. Heinen, *Phys. Rev. Lett.*, 2012, **109**, 048302.
56 S. B. Debord and L. A. Lyon, *J. Phys. Chem. B*, 2003, **107**, 2927–2932.
57 G. Romeo and M. P. Ciamarra, *Soft Matter*, 2013, **9**, 5401–5406.
58 G. Romeo, L. Imperiali, J. Kim, A. Fernández-Nieves and D. A. Weitz, *J. Chem. Phys.*, 2012, **136**, 124905.
59 X. Xia, Z. Hua and M. Marquez, *J. Controlled Release*, 2005, **103**, 21–30.
60 J. Zhou, G. Wang, L. Zou, L. Tang, M. Marquez and Z. Hu, *Biomacromolecules*, 2008, **9**, 142–148.
61 Z. Xing, C. Wang, J. Yan, L. Zhang, L. Li and L. Zha, *Colloid Polym. Sci.*, 2010, **288**, 1723–1729.
62 X. Liu, H. Guo and L. Zha, *Polymers*, 2012, **61**, 1144–1150.
63 E. Siband, Y. Tran and D. Hourdet, *Macromolecules*, 2011, **44**, 8185–8194.
64 V. Nigro, R. Angelini, M. Bertoldo and B. Ruzicka, *Colloids Surf., A*, 2017, DOI: 10.1016/j.colsurfa.2017.04.059.
65 H. Shirota and K. Horie, *Macromol. Symp.*, 2004, **207**, 79–93.
66 V. Tudisca, M. Ricci, R. Angelini and B. Ruzicka, *RSC Adv.*, 2012, **2**, 11111.
67 F. A. de Melo Marques, R. Angelini, E. Zaccarelli, B. Farago, B. Ruta, G. Ruocco and B. Ruzicka, *Soft Matter*, 2015, **11**, 466–471.
68 F. A. de Melo Marques, R. Angelini, G. Ruocco and B. Ruzicka, *J. Phys. Chem. B*, 2017, **121**, 4576–4582.
69 R. Kohlrausch, *Pogg. Ann. Phys. Chem.*, 1854, **91**, 179–214.
70 G. Williams and D. C. Watts, *J. Chem. Soc., Faraday Trans.*, 1970, **66**, 80–85.
71 J. Colmenero, A. Alegría, J. M. Alberdi, F. Alvarez and B. Frick, *Phys. Rev. B: Condens. Matter Mater. Phys.*, 1991, **44**, 7321–7329.
72 J. Colmenero, A. Alegría and A. Arbe, *Phys. Rev. Lett.*, 1992, **69**, 478–481.
73 C. Scherzinger, O. Holderer, D. Richter and W. Richtering, *Phys. Chem. Chem. Phys.*, 2012, **14**, 2762–2768.
74 P. Flory, *Principles of Polymer Chemistry*, Cornell University, Ithaca, New York, 1953.
75 B. Erman and P. J. Flory, *Macromolecules*, 1986, **19**, 2342–2353.
76 T. Lòpez-Leòn and A. Fernandez-Nieves, *Phys. Rev. E: Stat., Nonlinear, Soft Matter Phys.*, 2007, **75**, 1–7.
77 R. Böhmer, K. L. Ngai, C. Angell and D. Plazek, *J. Chem. Phys.*, 1993, **99**, 4201–4209.
78 A. J. Banchio and G. Nagägele, *J. Chem. Phys.*, 2008, **128**, 104903.
79 J. Gapinski, A. Patkowski, A. J. Banchio, J. Buitenhuis, P. Holmqvist, M. P. Lettinga, G. Meier and G. Nagägele, *J. Chem. Phys.*, 2009, **130**, 084503.
80 J. Gapinski, A. Patkowski, A. J. Banchio, P. Holmqvist, G. Meier, M. P. Lettinga and G. Nagägele, *J. Chem. Phys.*, 2007, **126**, 104905.